34th Annual International Conference of the IEEE EMBS
San Diego, California USA, 28 August - 1 September, 2012

Instantaneous Heart Rate Detection Using Short-Time Autocorrelation for Wearable Healthcare Systems*

Masanao Nakano, Toshihiro Konishi, Shintaro Izumi, Hiroshi Kawaguchi, and Masahiko Yoshimoto,
Members, IEEE

Abstract— **This report describes a robust method of Instantaneous Heart Rate (IHR) detection from noisy electrocardiogram (ECG) signals. Generally, the IHR is calculated from the interval of R-waves. Then, the R-waves are extracted from the ECG using a threshold. However, in wearable biosignal monitoring systems, various noises (e.g. muscle artifacts from myoelectric signals, electrode motion artifacts) increase incidences of misdetection and false detection because the power consumption and electrode distance of the wearable sensor are limited to reduce its size and weight. To prevent incorrect detection, we use a short-time autocorrelation technique. The proposed method uses similarity of the waveform of the QRS complex. Therefore, it has no threshold calculation Process and it is robust for noisy environment. Simulation results show that the proposed method improves the success rate of IHR detection by up to 37%.**

I. Introduction

A growing interest exists in wearable biosignal monitoring systems. Biosignal measurements during daily life at home are important for us to ascertain our health condition [1]. This report specifically describes IHR detection from noisy ECG signals for a wearable ECG monitoring system. The IHR is an important biosignal that is useful for heart disease detection, heart rate variation (HRV) analysis [2], and exercise intensity estimation [3].

The key factor affecting wearable system usability is miniaturization and weight reduction. A wearable and wireless ECG telemetry system [4, 5] and single-chip ECG monitoring system LSIs [6, 7, 8] have been developed. However, the wearable ECG monitor is sensitive to noise because its electrodes are close together. Especially, if a subject is not at rest (e.g. during exercise), the signal-to-noise ratio (SNR) of ECG signals will be degraded.

In general, to prevent SNR degradation, sophisticated analog front-end circuits are necessary. The analog front-end of the ECG monitoring system consists mainly of amplifiers, analog filters, and an analog to digital converter (ADC). Unfortunately, analog circuits have high power-consumption and area. The battery weight is dominant in the wearable system. Therefore, the battery capacity and power consumption must be reduced for weight reduction.

The amplifier has a tradeoff between the power consumption and its performance (e.g., gain, phase characteristic, common mode rejection ratio). Moreover, the analog filter in ECG monitor has a large RC time constant because the frequency range of ECG signals is low ($f < 1$ kHz). Consequently, it is difficult to use a high performance amplifier and analog filters, which have a high quality factor.

However, ultra-low-power ADCs, which have sub-uW power consumption and limited sample rate, are developed for biomedical applications [9, 10]. Furthermore, according to Moore's law, a power of digital portions is scaled down with the progress of Process technology. In contrast, the power consumption of analog circuits will not scale at the same rate as that of digital circuits. Therefore, the feature and purpose of our approach is digital signal Processing to reduce the performance requirements of the analog portion and minimize the power consumption of the entire system.

II. Conventional Method

Extracting R-waves with a threshold determination is a general approach for IHR detection from ECG. Recently, more robust IHR detection approaches have been proposed such as using a wavelet transform [11], artificial neural networks [12], a root-mean-square threshold determination [13], and adaptive filtering [14]. However, these methods have a threshold determination Process. Thereby, misdetections and false detections increase drastically in noisy conditions.

A wavelet transform with quadratic spline wavelet (QSW) has been used in several robust ECG monitoring systems [7]. The QSW requires a small amount of calculation and hardware cost because it can be implemented using only adders and shift operators. Fig. 1 presents frequency characteristics of the QSW. The sampling rate is 128 Hz, and the pass band is from 10 Hz to 30 Hz. Fig. 2 depicts the ECG and well-known noise waveforms.

Figs. 1 and 2 show that the base-line wander and hum noise can be removed easily using QSW or other digital filters. However, unfortunately, the frequency range of the muscle artifact and electrode motion artifact is similar to the desired ECG signals. Consequently, if a subject is not at rest (e.g. during exercise) and the SNR is low, it is difficult to extract the R-waves.

* Research supported by Ministry of Economy, Trade and Industry (METI) and the New Energy and Industrial Technology Development Organization (NEDO).

M. Nakano, T. Konishi, S. Izumi, H. Kawaguchi, and M. Yoshimoto are with Kobe University, 1-1-Rokkodai Nada Kobe Hyogo Japan (corresponding author to provide phone: 078-803-6629; fax: 078-803-6629; e-mail: nakano@cs28.cs.kobe-u.ac.jp).

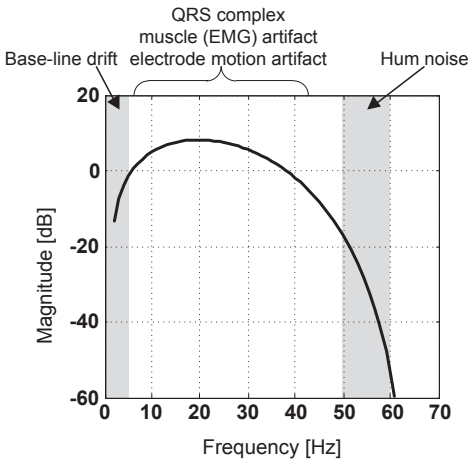

Figure 1. Frequency characteristics of QSW.

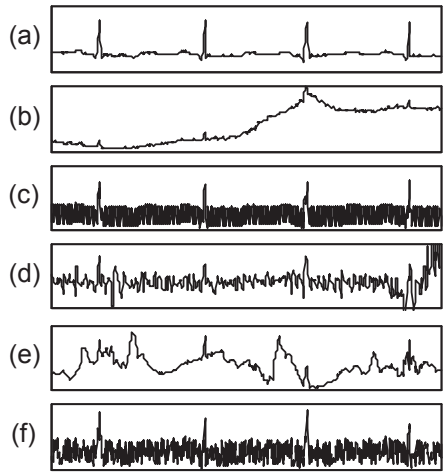

Figure 2. Waveform examples of (a) electrocardiogram with (b) baseline wander, (c) hum noise, (d) muscle artifact, (e) electrode motion artifact, and (f) white noise.

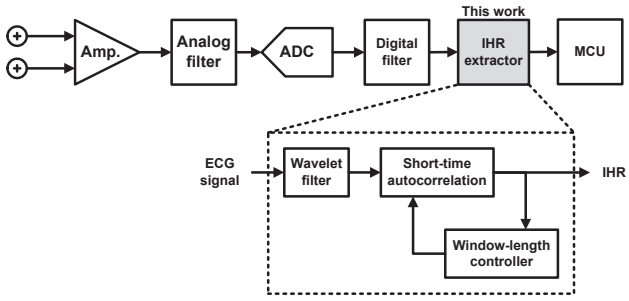

Figure 3. Block diagram of the proposed system.

III. Proposed Method

A. System Overview

We specifically examined an autocorrelation method [15] for IHR detection that uses similarity of the QRS complex's waveform. Therefore, the autocorrelation is effective for noise containing muscle artifacts and electrode motion artifacts.

As shown in Fig. 3, the proposed method comprises three components: a QSW filter, a short-time autocorrelation, and a window-length controller. The sampling rate of input ECG signals is set to 128 Hz, and the output rate of IHR is set to 1 Hz.

Previously, autocorrelation was used in a non-invasive monitoring system [16]. However, this method requires numerous computations because it calculates the average heart-rate in a long duration (e.g. 30 s). In contrast, our proposed method calculates the short-time autocorrelation to obtain accurate IHR with few computations.

B. Short-time Autocorrelation

Fig. 4 and Eq. (1) show that the short-time autocorrelation is calculated to detect IHR from the output signal of QSW filter ($x[t]$). In Fig. 4, *IHR[n]* denotes the nearest RR interval at time t_n, L_{window} denotes the length of a search window, t_{shift} denotes the window shift length, and $t_{\text{offset}}[t_n]$ signifies the time length from a nearest R-peak to t_n. The heart rate of a healthy subject is from 40 bpm to 220 bpm. Therefore, the value of t_{shift} is set from 0.273 s to 1.5 s.

$$IHR[n] = \max_{0.273 \le t_{shift} \le 1.5} \left\{ C(t_{shift}) \cdot \sum_{\tau=0}^{L_{window}} x[t_n - \tau] \cdot x[(t_n - t_{shift}) - \tau] \right\} \quad (1)$$

In eq. (1), $C(t_{\text{shift}})$ denotes the weight constant. To choose the recent peak of the correlation coefficient from time t_n, C is set as presented below.

$$C(t_{shift}) = \begin{cases} 1 & (t_{shift} < 0.546) \\ 0.75 & (0.546 \le t_{shift} < 0.983) \\ 0.5 & (0.983 \le t_{shift}) \end{cases}$$

Then, the range of t_{shift} is determined by the maximum rate of beat-to-beat variation, which is generally 20% in a healthy subject [17]. If we must address larger variation than 20%, then a longer range of t_{shift} is necessary.

The time interval of the IHR calculation depends on applications, and the total amount of computations is inversely proportional to the time interval. For this study, the time interval is set to 1 s because the HRV analysis requires up to 0.5 Hz frequency components [2].

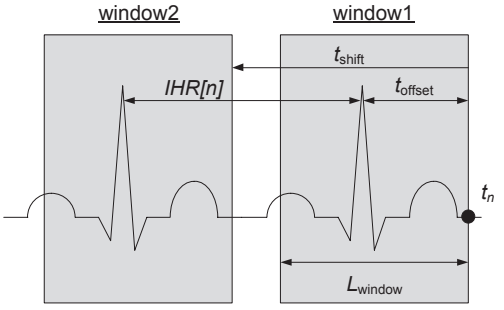

Figure 4. Short-time autocorrelation for IHR detection.

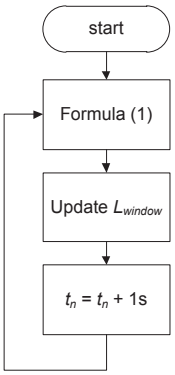

Figure 5. Flow chart of the proposed method.

C. Window-length optimization

The control parameter L_{window} is updated according to the estimated IHR. To obtain the IHR from eq. (1), at least one R-wave is included in window 1. However, if the L_{window} is adjusted to the minimum length with one R-wave, then the computational amount and the accuracy of estimated IHR will be improved.

To realize the adaptive L_{window} optimization, L_{window} must be set to longer than the maximum length of t_{offset} [t_n]. If the $IHR[n\text{-}1]$ is smaller than 0.316 s, then three R-waves exist between t_n-1 and t_n at maximum. Consequently, the worst case of t_{offset} [t_n] is $IHR[n\text{-}1] \times (1.2)^3$ because the maximum beat-to-beat variation is 20%. Similarly, if the $IHR[n\text{-}1]$ is 0.316–0.695 s, then the maximum value of t_{offset} [t_n] is $IHR[n\text{-}1] \times (1.2)^2$. If the $IHR[n\text{-}1]$ is larger than 0.695 s, then t_{offset} [t_n] is up to $IHR[n\text{-}1] \times (1.2)$. Therefore, L_{window} can be given as presented below.

$$L_{window} = \begin{cases} IHR[n-1]\cdot(1.2)^3 & (IHR[n-1] < 0.316) \\ IHR[n-1]\cdot(1.2)^2 & (0.316 \le IHR[n-1] < 0.695) \\ IHR[n-1]\cdot(1.2) & (0.695 \le IHR[n-1]) \end{cases}$$

Fig. 5 shows a flow chart of the proposed method. Unfortunately, the computational cost of the proposed method is about one hundred times as great as that for general threshold methods. However, this method can be implemented in the digital domain. We estimate that the power consumption of the proposed method is one-tenth that of the analog portion, which includes an instrumental amplifier, analog filter, and ADC. Furthermore, the power consumption of the analog portion will be reduced using the proposed method because it has high tolerance for noise. Therefore, the total power consumption of the wearable monitor can be reduced.

IV. Performance Evaluation

To verify the effects of the proposed method, we performed simulation experiments using MATLAB. In the simulation, the proposed method is compared to the threshold-based IHR detection method [6, 13].

First, we evaluate the accuracy of estimated IHR and noise tolerance using the public ECG database (MIT-BIH arrhythmia database [18]) and the noise database (MIT-BIH noise stress test database [19]). Fig. 6 shows the relation between the intensity of muscle artifact noise and the success rate of IHR detection. Here, Conv. 1 shows conventional threshold based methods using QSW [11] with RMS [13]. The second conventional method (Conv. 2 in Fig. 6) uses a derivative-based algorithm [6].

The SNR is calculated as shown below.

$$SNR = 20 \cdot \log_{10} \frac{x_{\max} - x_{\min}}{\sqrt{\frac{1}{N}\sum_{i=1}^{N}(x_i - y_i)^2}}$$

Then, x_i denotes the original ECG signal and y_i signifies the noise applied ECG signal. The $x_{\max}$, $x_{\min}$, and N respectively denote the maximum value of x_i, the minimum value of x_i, and the data length.

Table 1 presents simulation results of absolute error, relative error, and the success rate (less than 5% relative error) with the muscle artifact, electrode motion artifact, and white noise. In Table 1, "Mean" is the mean value of the absolute errors and "P_{90}" is the spread of errors is computed using the 90th percentile of the errors [20].

Simulation results show that the proposed method has high accuracy despite its use in a noisy condition. From Fig. 6, the noise tolerance with the muscle artifact is improved about 5.6 dB at the 95% success rate compared with the second conventional method [6].

Next, we evaluate the success rate using a measured ECG waveform obtained using a wearable ECG monitoring system (WHS-1; Union Tools Co. [21]). Fig. 7 shows the success rate comparison in a resting condition and during exercises (push-ups, sit-ups, and running). Then, the data length is 30 s in each condition. Fig. 8 portrays an example of a measured waveform during push-up. The sensor is pasted to the chest. Therefore, an intensive myoelectric signal caused by the muscle of chest is mixed into the ECG signal. The proposed method achieves success rate improvement of up to 37%.

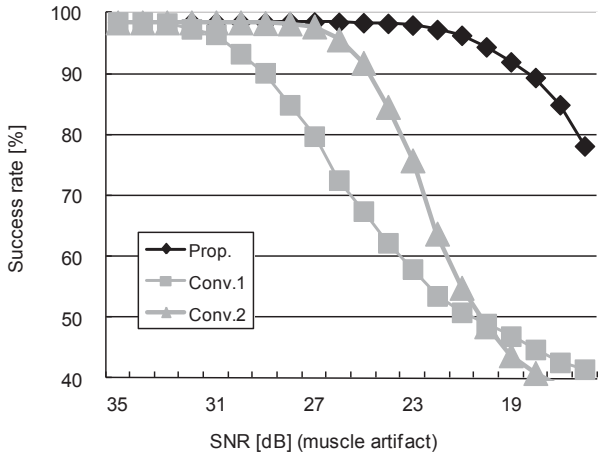

Figure 6. Relation between the muscle artifact noise intensity and the success rate.

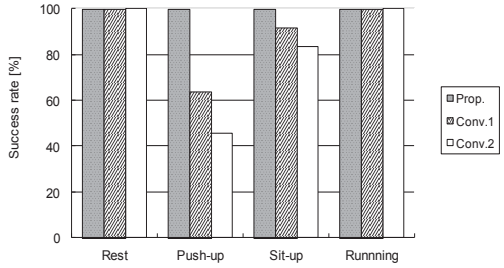

Figure 7. Comparison of IHR detection success rate with measured ECG.

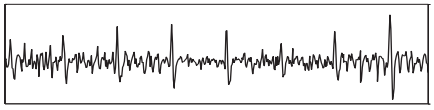

Figure 8. Example of measured ECG waveform during push-up exercise.

TABLE I. SIMULATION RESULTS

Noise	SNR [dB]	Absolute error [ms]				Relative error [%]				Success rate [%]	
		Mean		P_{90}		Mean		P_{90}			
		Prop.	Conv.2	Prop.	Conv.2	Prop.	Conv.2	Prop.	Conv.2	Prop.	Conv.2
muscle artifact	35	5.3	7.4	7.8	15.6	0.7	0.9	1.1	2.0	98.5	98.4
	30	5.5	7.4	7.8	15.6	0.7	0.9	1.1	2.0	98.4	98.4
	25	5.5	33.6	7.8	31.3	0.7	4.3	1.1	3.7	98.4	91.8
	20	14.0	231	15.6	532	1.8	29.5	2.0	66.1	94.4	48.5
electrode motion artifact	35	4.9	7.4	7.8	15.6	0.6	0.9	1.1	2.0	98.5	98.4
	30	5.0	8.4	7.8	15.6	0.6	1.1	1.1	2.0	98.6	98.1
	25	5.1	37.6	7.8	39.1	0.6	4.8	1.1	4.8	98.5	90.1
	20	17.1	176	23.4	508	2.2	22.7	3.0	65.1	91.6	56.5
white noise	35	5.3	7.5	7.8	15.6	0.7	0.9	1.1	2.0	98.4	98.4
	30	6.2	508	7.8	555	0.8	64.9	1.1	67.0	98.0	0.0
	25	101	508	336	555	12.9	64.9	42.6	67.0	63.3	0.0
	20	317	508	477	555	40.4	64.9	60.4	67.0	7.8	0.0

V. CONCLUSION

As described in this paper, we proposed a robust IHR detection algorithm using short-time autocorrelation. Simulation results show that the proposed method improves IHR accuracy despite its use in noisy conditions. The noise tolerance with the muscle artifact is improved 5.6 dB at the 95% success rate. The proposed method can contribute to the power and area reduction of the wearable biosignal monitoring system because it can be processed digitally.

REFERENCES

[1] H. Nakajima, T. Shiga, "Systems Health Care," In *Proc. of IEEE SMC*, pp.1167-1172, Oct. 2011.

[2] W. Roel, M. John, "Comparing Spectra of a Series of Point Events Particularly for Heart Rate Variability Data," *IEEE Trans. Biomed. Eng.*, BME-31, no.4, pp.384-387, Apr. 1984.

[3] S. Yazaki, T. Matsunaga, "Evaluation of activity level of daily life based on heart rate and acceleration," In *Proc. of SICE*, pp.1002-1005, Aug. 2010.

[4] K. Itao, T. Umeda, G. Lopez, M. Kinjo, "Human Recorder System Development for Sensing the Autonomic Nervous System," In *Proc. of IEEE Sensors*, pp.423-426, Oct. 2008.

[5] K. Itao, T.Ito, "Integrated Sensing Systems for Health and Safety," In *Proc. of DTIP Symposium*, pp.212-216, May 2011.

[6] H. Kim, R. F. Yazicioglu, S.Kim, et al., "A configurable and low-power mixed signal SoC for portable ECG monitoring applications," *VLSI Symp.*, pp.142-143, Jun. 2011.

[7] S. Y. Hsu, Y. L. Chen, P. Y. Chang, et al., "A Micropower Biomedical Signal Processor for Mobile Healthcare Applications," In *Proc. of IEEE ASSCC*, pp.301-304, Nov. 2011.

[8] M. Ashouei, J. Hulzink, M. Konijnenburg, et al., "A voltage-scalable biomedical signal Processor running ECG using 13 pJ/cycle at 1 MHz and 0.4V," *IEEE ISSCC Dig. Tech. Papers*, pp.332-334, Feb. 2011.

[9] M. van Elzakker, E. van Tuijl, P. Geraedts, et al., "A 1.9 uW 4.4 fJ/Conversion-Step 10 b 1 MS/s Charge - Redistribution ADC," IEEE Journal of Solid-State Circuits, vol. 45, no. 5, pp.1007-1015, May 2010.

[10] P. Harpe, Y. Zhang, G. Dolmans, et al., "A 7-to-10b 0-to-4 ms/s Flexible SAR ADC With 6.5-to-16fJ/conversion-step," *IEEE ISSCC Dig. Tech. Papers*, pp.472-473, Feb. 2012.

[11] C. I. Ieong, M. I. Vai, P. U. Mak, P. I. Mak, "ECG Heart Beat Detection via Mathematical Morphology and Quadratic Spline Wavelet Transform," In *Proc. of IEEE ICCE*, pp.609-610, Jan. 2011.

[12] Q. Xue, Y.H.Hu, W. J. Tompkins, "Neural – network - based adaptive matched filtering for QRS detection," *IEEE Tran. Biomed. Eng.*, vol.39, no.4, pp.317-329, Apr. 1992.

[13] J. P. Martinez, R. Almeida, S. Olmos, et al., "A wavelet-based ECG delineator: evaluation on standard databases," *IEEE Trans. Biomed. Eng.*, vol.51, no.4, pp.570-581, Apr. 2004.

[14] P. S. Hamilton, W. J. Tompkins, "Adaptive matched filtering for QRS detection," In *Proc. of IEEE EMBC*, vol.1, pp.147-148, Nov. 1988.

[15] Y. Takeuchi, M. Hogaki, "An adaptive correlation ratemeter: a new method for Doppler fetal heart rate measurements," *Ultrasonics*, pp.127-137, May 1978.

[16] M. Sekine, K. Maeno, "Non-Contact Heart Rate Detection Using Periodic Variation in Doppler Frequency," In *Proc. of IEEE SAS*, pp.318-322, Feb. 2011.

[17] M. Malik, "Heart Rate Variability; standards of Measurement, Physiological Interpretation, and Clinical Use," *Circulation*, 1996; 93: 1043-1065.

[18] MIT-BIH Arrhythmia Database(mitdb), Record 100, "http://www.physionet.org/physiobank/database/mitdb/ "

[19] MIT-BIH Noise Stress Test Database(nstdb), "http://www.physionet.org/physiobank/database/nstdb/"

[20] C. Bruser, K. Stadlthanner, S. D. Waele, S. Leonhardt, "Adaptive Beat-to-Beat Heart Rate Estimation in Ballistocardiograms," *IEEE Trans.Inf. Technol. Biomed.*, vol.15, no.5, pp.778-786, Sep. 2011.

[21] UNION TOOL, "http://www.uniontool.co.jp/english/index.html"